NEOPLASIA
www.neoplasia.com

Volume 11 Number 1 January 2009 pp. 57–65 57

Oncogenic Activation of MAP Kinase by *BRAF* Pseudogene in Thyroid Tumors[1]

Minjing Zou*, Essa Y. Baitei*, Ali S. Alzahrani†, Futwan Al-Mohanna‡, Nadir R. Farid§, Brian Meyer* and Yufei Shi*

*Department of Genetics, King Faisal Specialist Hospital and Research Centre, P.O. Box 3354, Riyadh 11211, Saudi Arabia; †Department of Biological and Medical Research, King Faisal Specialist Hospital and Research Centre, P.O. Box 3354, Riyadh 11211, Saudi Arabia; ‡Department of Medicine, King Faisal Specialist Hospital and Research Centre, P.O. Box 3354, Riyadh 11211, Saudi Arabia; §Osancor Biotech Inc, Watford, Herts WD17 4EJ, UK

Abstract

Activating *BRAF* mutations have been reported in 40% of papillary thyroid carcinomas (PTCs). The involvement of *BRAF* pseudogene in thyroid tumorigenesis has not previously been studied. We investigated *BRAF* pseudogene expression in 68 thyroid tumors: 16 multinodular goiters, 43 classic PTCs, 6 follicular variants of PTC, and 3 anaplastic thyroid carcinomas. *BRAF* pseudogene function was studied by Western blots, soft agar assay, and tumorigenesis in nude mice. *BRAF* pseudogene expression was detected in 7 multinodular goiters, 18 classic PTC, and 1 follicular variants of PTC. There is an inverse correlation between *BRAF* pseudogene expression and *BRAF* mutation. The pseudogene transcripts were more frequently detected in tumors without *BRAF* mutation than those with *BRAF* mutation. Furthermore, *BRAF* pseudogene expression could activate the MAP kinase signaling pathway, transform NIH3T3 cells *in vitro*, and induce tumors in nude mice. These data suggest that *BRAF* pseudogene activation may play a role in thyroid tumor development.

Neoplasia (2009) 11, 57–65

Introduction

Papillary thyroid carcinomas (PTCs) are the most common type of differentiated thyroid carcinomas, accounting for some 85% thyroid malignancies [1]. The most common genetic events are involved in RAS-RAF-MEK-ERK-MAPK signaling pathway such as *RAS* point mutations, *RET/PTC* oncogenes, *NTRK1* rearrangements (TRK), and *BRAF* mutations [2–8]. *BRAF* is a serine/threonine kinase that serves as an immediate downstream effector of RAS in the RAS-RAF-MEK-ERK-MAPK signaling cascade. Oncogenic mutations in *BRAF* are common in human cancers, nearly all of which are the T1799A transversion in exon 15, resulting in a V600E substitution in the protein [9,10]. This mutation is believed to produce a constitutively active kinase by disrupting hydrophobic interactions between residues in the activation loop and residues in the ATP binding site [11,12].

Two human *BRAF* loci (B-raf-1 and B-raf-2) have been identified [13]. B-raf-1 is located on chromosome 7q34 and encodes the functional 94-kDa BRAF protein. B-raf-2 is located on chromosome Xq13 and has been predicted to be an inactive processed pseudogene owing to the presence of point mutations, insertions, and deletions relative to B-raf-1, although its expression and function has not been investigated yet [13].

Pseudogenes have a similar DNA sequence to their functional genes; they are nonetheless unable to produce functional final protein products and have generally been considered as evolutionary "dead-end." They may originate from reverse transcription (RT) of normal mRNA transcripts (processed pseudogenes) or from gene duplication (nonprocessed pseudogenes) [14]. One of the interesting findings from genome sequencing is the abundance of pseudogenes in mammalian genomes: roughly the same number of pseudogenes as protein-coding

Address all correspondence to: Yufei Shi, MBC 3, Department of Genetics, King Faisal Specialist Hospital and Research Centre, P.O. Box 3354, Riyadh 11211, Saudi Arabia. E-mail: yufei@kfshrc.edu.sa

[1]The research was funded by King Faisal Specialist Hospital and Research Centre (grant no. 2070064) and King Abdulaziz City for Science and Technology (grant no. ARP-24-11).

Received 27 August 2008; Revised 12 October 2008; Accepted 14 October 2008

DOI 10.1593/neo.81044

genes in all mammals sequenced so far [15]. Now there is a growing number of evidence suggesting that some of them may have active regulatory roles [16–18].

In the present study, we investigated *BRAF* pseudogene expression in 68 thyroid tumors from Saudi Arabia, its relationship with *BRAF* mutation, and its association with clinical and pathological features of PTC. The functional aspects of *BRAF* pseudogene expression were also studied.

Materials and Methods

Thyroid Tumor Specimens

All tumor tissues were obtained at surgery and stored at −70°C until processed. The clinical staging of thyroid cancer was based on the TNM classification [19]. Sixty-eight thyroid tumors were studied: 16 benign multinodular goiters, 43 classic PTCs, 6 follicular variants of PTC, and 3 anaplastic thyroid carcinomas (ATCs). The study was reviewed and approved by the institutional review board.

DNA Amplification and Sequence Analysis of Exon 15 of BRAF

Tumor DNA was extracted by standard proteinase-K treatment followed by phenol/chloroform extraction. Exon 15 was amplified by polymerase chain reaction (PCR) using the following two primers: 5′-TCATAATGCTTGCTCTGATAGGA-3′ and 5′-CTAGTAACTCAGCAGCATCTC-3′. The PCR conditions were 95°C for 10 minutes followed by 35 cycles of amplification (95°C for 1 minute, 54°C for 1 minute, and 72°C for 1 minute). The resulting PCR products were analyzed by gel electrophoresis. Each successfully amplified fragment was directly sequenced using the BigDye Terminator V3.1 Cycle Sequencing kit (Applied Biosystems, Foster City, CA).

Reverse Transcription–PCR Analysis of BRAF *Pseudogene Transcripts*

Total RNA was extracted using the guanidinium thiocyanate–phenol–chloroform method. To amplify *BRAF* pseudogene transcripts, 2 μg of total RNA were first treated with DNase 1 (10 U at 37°C for 30 minutes, heat inactivation at 70°C for 5 minutes) to remove contaminating genomic DNA and then reverse-transcribed into cDNA using Oligo dT–based reverse transcription system (Proems, Madison, WI). Pseudogene transcripts were amplified by PCR using the following two specific primers: 5′-CTTGTAT**T**ACC**T**TCTCCATAT**A**-3′ and 5′-CTAGACCAAAATCACCTATTT**CC**-3′. The sequences different from *BRAF* wild type gene were highlighted in bold. Polymerase chain reaction conditions were the same as described above. The resulting 185-bp PCR products were analyzed by gel electrophoresis and were directly sequenced to confirm specificity of pseudogene transcripts. To amplify *BRAF* transcripts covering exon 15, the forward primer (based on exon 14: 5′-GCATGGATTACTTACACGCCA-3′) and the reverse primer (based on exon 16: 5′-CAATTCATACAGAACAATCC-3′), were located in different exons to avoid amplification of contaminating genomic DNA. This primer pair can also amplify corresponding *BRAF* pseudogene transcripts.

Quantitative Real-time RT-PCR Analysis of BRAF *Transcripts*

Quantitative RT-PCR analysis was performed as described previously [20]. Briefly, total RNA were reverse-transcribed into cDNA. LightCycler DNA Master SYBR Green kit was used for quantitative PCR analysis (Roche, Mannheim, Germany). The cDNA mix was diluted 10-fold, and 2 μl of the dilution was used for real-time PCR analysis. *BRAF*-specific PCR primers for 216-bp cDNA fragment were 5′-CAAACTTATAGATATTGCAC**A**-3′ (sense) and 5′-TCTGGTGCCAT**C**CACAAAA**TG**-3′ (antisense). The sequence different from *BRAF* pseudogene was highlighted in bold, and the PCR primers span intron 14 so that contaminating genomic DNA will not be amplified. The mRNA level of housekeeping gene glyceraldehydes-3-phosphate dehydrogenase (*GAPDH*) was used as an internal control, and a 300-bp PCR product was amplified using the following two primers: 5′-ACAGTCAGCCGCATCTTCTT-3′ (sense) and 5′-TTGATTTTGGAGGGATCTCG-3′ (antisense). The PCR conditions were as follows: 95°C for 30 seconds followed by 35 cycles of amplification (95°C for 5 seconds, 48°C for 5 seconds, and 72°C for 10 seconds). The resulting concentrations of *BRAF* PCR products were normalized by comparison with *GAPDH* and were used to determine the *BRAF* mRNA level.

Cloning and Expression of BRAF*–Wild Type, –V600E Mutant, and –Pseudogene*

The full-length *BRAF*–wild type and –V600E mutant cDNA were amplified by RT-PCR from total RNA extracted from thyroid tissue using the following primers: 5′-GACAGCGGCCGCTCGGGCCC-3′ (sense), 5′-TCTCGGTTATAAGATGGCGGCG-3′ (sense, internal for nested PCR), and 5′-CCTGAACTCT CTCACTCATTTG-3 (antisense). The pseudogene cDNA was amplified by RT-PCR using primers corresponding to exon 2 (5′-GTATGGAATATCAAACAAATAA-3′) and 3′untranslated region of wild type *BRAF*: 5′-CCTGAACTCTCTCACTCATTTG-3 (internal for nested PCR, antisense) and 5-TCCTTTTGTTGCTACTCTCCTG-3′ (antisense). The resulting cDNA fragment was cloned into the expression vector pcDNA3.1, which is under the control of the CMV promoter (Invitrogen, Carlsbad, CA), and was verified by DNA sequencing with no mutation found. All three constructs (pBRAF^{WT}, pBRAF^{V600E}, and pBRAF^{PSEUDO}) were transfected into CHO and NIH3T3 cells using Lipofectamine (Invitrogen). Cells were selected in the presence of 400 μg/ml G418 for 3 weeks (Sigma, St. Louis, MO), and stable clones were pooled for experiments. To detect protein expression of the pseudogene transcripts, the coding sequence was amplified by PCR from the pseudogene cDNA and cloned into a pcDNA3.1/V5-His expression vector in frame with the V5 epitope at the C-terminus (Invitrogen), using the following two primers: 5′-GGAACGGAACTGATTTTTCT GTT-3′ (sense) and 5′-GTGATCTTCATCTGCTGGT CGGAA-3′ (antisense). The resulting plasmid (pBRAF$^{PSEUDO\text{-}V5}$) was stably transfected into CHO cells.

Western Blot Analysis

A total of 60 μg of protein from stably transfected CHO cells (pBRAF$^{PSEUDO\text{-}V5}$, pBRAF^{WT}, pBRAF^{V600E}, and pBRAF^{PSEUDO}) were loaded onto a 12% sodium dodecyl sulfate–polyacrylamide gel. Proteins were transferred to a polyvinylidene fluoride membrane and were subjected to Western blot analysis with anti-V5 monoclonal antibody (1:5000 dilution; Invitrogen) or anti–total ERK 1/2 (1:2000 dilution) and anti–phospho-ERK 1/2 antibodies (1:1000; Santa Cruz Biotechnology Inc., Santa Cruz, CA).

Quantification of MAP Kinase Activation by BRAF *Pseudogene in CHO Cells*

pBRAF^{PSEUDO}– and pBRAF$^{PSEUDO\text{-}V5}$–transfected CHO cells were cultured in serum-free medium for 16 hours. The cells were

then stimulated with 20% fetal bovine serum for 2 hours in the presence or absence of 20 μM MEK inhibitor U0126 or BRAF inhibitor SB590885 (EMD Chemicals, Inc., Gibbstown, NJ) for 2 hours. The amount of cellular phospho-ERK 1/2 was measured using a cell-based ELISA kit according to the manufacturer's instructions (SuperArray Bioscience Co., Frederick, MD).

Transformation Assays

A total of 2×10^4 stably transfected NIH3T3 cells ($pBRAF^{WT}$, $pBRAF^{V600E}$, and $pBRAF^{PSEUDO}$) were plated into a six-well cell culture plate for an anchorage-independent growth by soft agar assay according to the manufacturer's instructions (Chemicon International, Temecula, CA). For *in vivo* transformation experiments, 1×10^6 of stably $pBRAF^{PSEUDO}$–transfected NIH3T3 cells were injected subcutaneously into four female nude mice (The Jackson Laboratory, Bar Harbor, ME). Mice were observed twice weekly and killed when tumor reached 5 × 5 mm in size.

Results

BRAF *Pseudogene Expression in Thyroid Tumors*

Because *BRAF* pseudogene is a retrogene and has no intron, contaminating genomic DNA will be amplified by PCR from RNA preparations. To eliminate genomic DNA contamination, RNA was first digested with DNase 1 before being reverse-transcribed into cDNA. The pseudogene transcripts were detected in 7 (43.8%) of 16 multinodular goiters, 18 (41.9%) of 43 classic PTCs, and 1 (16.7%) of 6 follicular variants of PTC (FVPTCs; Figure 1 and Table 1). The transcripts were not detected in five normal thyroid tissues (data not shown). The transcripts were detected more frequently in tumors without *BRAF* mutation (20/27, 74.4%) than those with *BRAF* mutation (7/27, 25.9%; Table 1; $P < .01$, Fisher exact test). They were

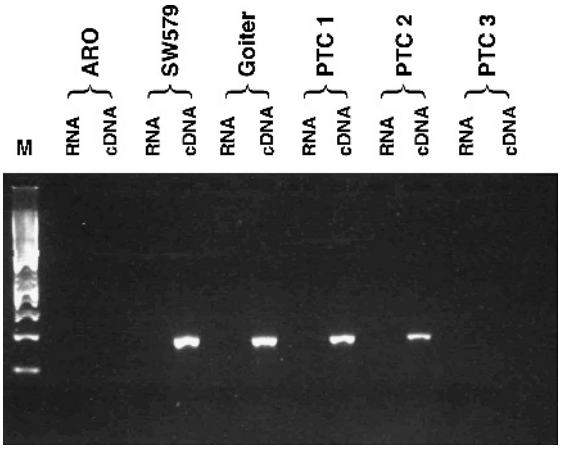

Figure 1. Detection of *BRAF* pseudogene expression by RT-PCR from thyroid tumor samples. A total of 2 μg of total RNA were first treated with DNase 1 to remove contaminating genomic DNA and then reverse-transcribed into cDNA. Pseudogene cDNA were amplified by PCR using specific primers. No amplification was seen when RNA was used as a template. Representative results from two cell lines and four samples were shown. Pseudogene transcripts were detected as a 185-bp cDNA fragment from SW579 cell line, one goiter and two PTC samples.

Table 1. *BRAF* T1799A Mutation and Pseudogene Expression in Thyroid Carcinoma.

No.	Diagnosis	Age (year)	Sex	Stage	*BRAF* T1799A Mutation	*BRAF* Pseudogene Expression
1	Goiter	35	F		No	No
2	Goiter	49	M		No	No
3	Goiter	40	F		No	Yes
4	Goiter	39	F		No	Yes
5	Goiter	38	F		No	Yes
6	Goiter	38	F		No	Yes
7	Goiter	30	F		No	No
8	Goiter	65	F		No	No
9	Goiter	31	F		No	No
10	Goiter	30	F		No	Yes
11	Goiter	38	F		No	Yes
12	Goiter	43	M		No	Yes
13	Goiter	60	F		No	No
14	Goiter	52	M		No	No
15	Goiter	21	F		No	No
16	Goiter	45	F		No	No
17	PTC	28	F	I	No	No
18	PTC	40	M	I	No	No
19	PTC	23	F	I	No	No
20	PTC	48	F	I	No	No
21	PTC	36	F	I	No	No
22	PTC	36	F	I	No	Yes
23	PTC	43	F	I	No	Yes
24	PTC	18	M	I	No	Yes
25	Metastatic PTC	33	F	1	No	No
26	Metastatic PTC	24	F	I	No	No
27	Metastatic PTC	35	F	I	Yes	No
28	Metastatic PTC	26	F	I	No	Yes
29	Metastatic PTC	36	F	I	Yes	Yes
30	Metastatic PTC	22	F	II	No	No
31	Metastatic PTC	41	F	II	Yes	Yes
32	Metastatic PTC	12	F	I	No	Yes
33	Metastatic PTC	40	F	I	Yes	No
34	Metastatic PTC	32	F	I	No	No
35	Metastatic PTC	24	F	I	No	Yes
36	Metastatic PTC	30	F	I	Yes	No
37	Metastatic PTC	25	F	I	Yes	No
38	Metastatic PTC	37	F	I	No	Yes
39	Metastatic PTC	26	M	I	No	Yes
40	PTC	82	M	II	Yes	Yes
41	PTC	57	F	II	Yes	Yes
42	PTC	52	F	II	No	Yes
43	Metastatic PTC*	27	F	II	No	Yes
44	PTC	55	F	III	Yes	Yes
45	PTC	46	M	III	No	No
46	PTC	60	M	III	Yes	No
47	PTC	58	F	III	No	No
48	PTC	73	F	III	Yes	No
49	PTC	72	F	III	No	No
50	PTC	59	F	III	Yes	No
51	PTC	50	M	III	Yes	No
52	PTC	72	F	III	Yes	No
53	PTC	66	M	III	Yes	No
54	PTC	71	M	IV	No	Yes
55	PTC	46	F	IV	Yes	Yes
56	PTC	70	F	IV	Yes	No
57	PTC	63	M	IV	Yes	No
58	PTC	49	M	IV	Yes	No
59	PTC	77	M	IV	Yes	Yes
60	ATC	81	M	IV	Yes	No
61	ATC	76	F	IV	Yes	No
62	ATC	43	F	IV	Yes	No
63	FVPTC	32	F	I	No	No
64	FVPTC	34	F	I	No	No
65	Metastatic FVPTC	21	F	I	No	Yes
66	FVPTC	43	M	I	No	No
67	FVPTC	68	F	IV	No	No
68	FVPTC	45	F	II	No	No
	ARO cell line				Yes	No
	NPA cell line				Yes	No
	SW579 cell line				No	Yes

Metastatic PTC refers to stage I or II tumors with local lymph note metastasis.
*PTC-1 mutation was detected.

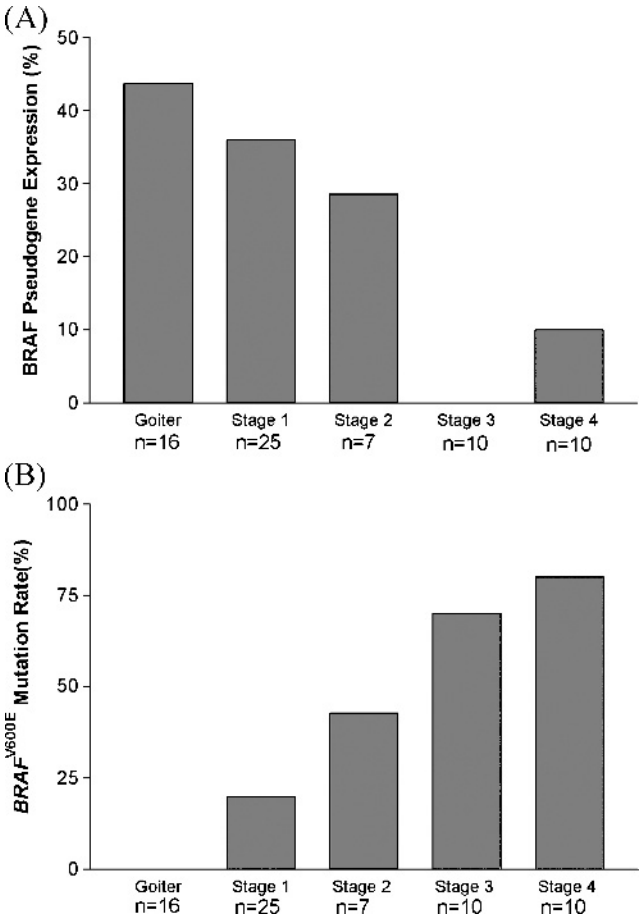

Figure 2. *BRAF* pseudogene expression in thyroid tumor specimens. (A) Inverse association of *BRAF* pseudogene expression with aggressiveness of PTC. The frequency of *BRAF* pseudogene expression was reduced in advanced stages of thyroid carcinoma. No *BRAF* pseudogene transcripts were detected in stage III PTC samples. (B) Association of *BRAF* mutation with aggressiveness of PTC. Higher frequency of V600E mutation was detected in advanced stages of thyroid carcinoma. Six FVPTC and three ATC samples were included in the analysis. No mutation was detected in the goiter.

also found more frequently in benign tumors and in early stages of thyroid cancer (Figure 2*A*). By contrast, *BRAF* mutation is frequently found in patients with stages III and IV tumors ($P < .01$; Figure 2*B*). When using generic primers surrounding *BRAF* exon 15, wild type and mutated T1799A *BRAF* transcripts could be detected together with pseudogene transcripts by RT-PCR sequence analysis (Figure 3). The pseudogene transcripts harbored several sequence variations compared with wild type *BRAF*: T1794C (A1794A), C1807T (R603X), C1848T (S616S), A1849T (I617F), G1857T (W619C), C1894T (P632S), and G1915A (V639I) (Figure 3). If one overlooks the existence of pseudogene expression, these sequence variations could be mistakenly identified as *BRAF* mutations. However, these sequence variations were not present in the matched genomic DNA (Figure 3) because *BRAF* and its pseudogene are located on chromosomes Xq13 and 7q34, respectively. Sequence analysis showed that the pseudogene transcripts were more abundant than wild type or mutant *BRAF* transcripts in some tumor samples, as demonstrated by a single homozygous peak in the sequence chromatogram, whereas in other samples, heterozygous peaks could be detected, showing both functional *BRAF* and *BRAF* pseudogene transcripts (Figure 3).

To determine whether there is a correlation between *BRAF* gene expression and *BRAF* pseudogene expression, we performed quantitative PCR comparing *BRAF* gene expression among normal, pseudogene-positive, and pseudogene-negative tumor samples. As shown in Figure 4, no correlation of *BRAF* expression was found between pseudogene-positive and pseudogene-negative tumors. In pseudogene-positive samples, the mean of *BRAF/GAPDH* ratio is 0.63 ± 0.43 compared with 0.44 ± 0.14 in pseudogene-negative tumors ($P > .05$, Student's *t* test). These data suggest that *BRAF* pseudogene expression may not regulate *BRAF* expression.

Activation of MAP Kinase by BRAF *Pseudogene Expression*

Analysis of the pseudogene cDNA sequence revealed that it has a long open reading frame of 244 amino acids and corresponds to the

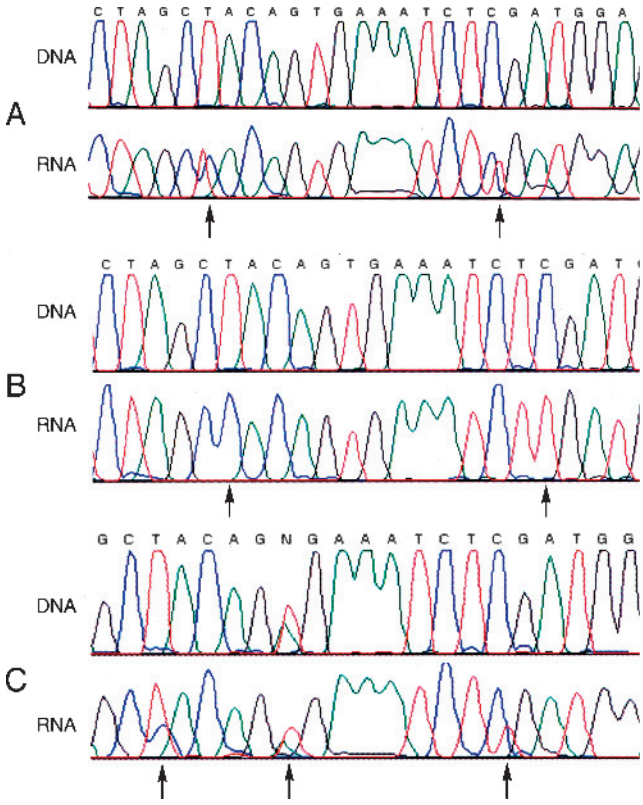

Figure 3. Detection of *BRAF* pseudogene transcripts by sequencing analysis of RT-PCR products. Three representative sequence chromatograms of matched DNA and RNA samples were shown. (A) Presence of both *BRAF* wild type and pseudogene transcripts in an RNA sample of multinodular goiter (no. 3 in Table 1). The pseudogene transcripts presented as heterozygous mutations at T1794C (A1794A) and C1807T (R603X), whereas matched DNA sample did not show the mutations. (B) Detection of only *BRAF* pseudogene transcripts in an RNA sample of multinodular goiter (no. 4 in Table 1). The pseudogene transcripts presented as homozygous mutations at T1794C (A1794A) and C1807T (R603X), whereas matched DNA sample did not show the mutations. (C) Presence of both *BRAF* mutant and pseudogene transcripts in an RNA sample of PTC (no. 44 in Table 1). The pseudogene transcripts presented as heterozygous mutations at T1794C (A1794A) and C1807T (R603X). Heterozygous T to A *BRAF* mutation was detected at nucleotide 1799 and was confirmed in the matched DNA sample.

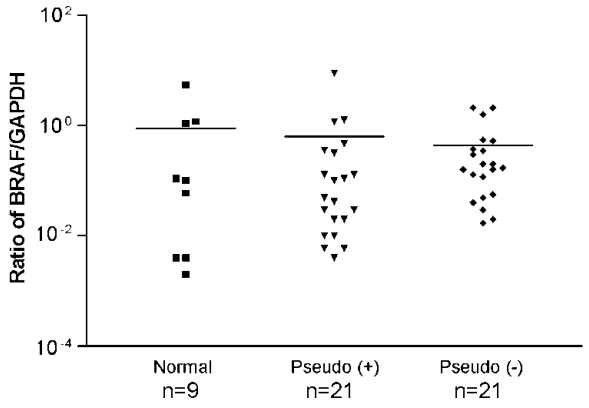

Figure 4. Real-time RT-PCR analysis of *BRAF* mRNA among normal, *BRAF* pseudogene-positive, and pseudogene-negative thyroid tumor samples. *BRAF* transcripts were quantified and normalized by comparison with *GAPDH*. Data are expressed as ratio of *BRAF*/*GAPDH* mRNA among different groups. Because *GAPDH* mRNA is more abundant than *BRAF*, log scale is used.

wild type CR1 domain (Figure 5), which has been shown to mediate autoinhibition of the C-terminal protein kinase domain (CR3) [21]. Amino acid sequence alignment between wild type *BRAF* and its pseudogene showed 85.7% homology, suggesting that they may interact with each other resulting in modulation of the MAP kinase signaling pathway. To further investigate the functional role of *BRAF* pseudogene expression, we cloned and expressed the pseudogene in both CHO and NIH3T3 cells. As shown in Figure 6*A*, *BRAF* pseudogene expression could activate MAP kinase in CHO cells. Similar results were also found in NIH3T3 cells. We next quantified MAP kinase activation by measuring phospho-ERK in *BRAF* pseudogene (full-length) and N-terminal part of *BRAF* pseudogene–transfected CHO cells. As shown in Figure 6*B*, both *BRAF* pseudogene and N-terminal part of *BRAF* pseudogene could induce a higher level of MAP kinase activation in the absence of serum stimulation. Both MEK inhibitor U0126 and *BRAF* inhibitor SB590885 could reduce the kinase activation by more than 70%. These data suggest that *BRAF* pseudogene could lead to constitutive MAP kinase activation through interaction with wild type BRAF and MEK, likely through

(A)

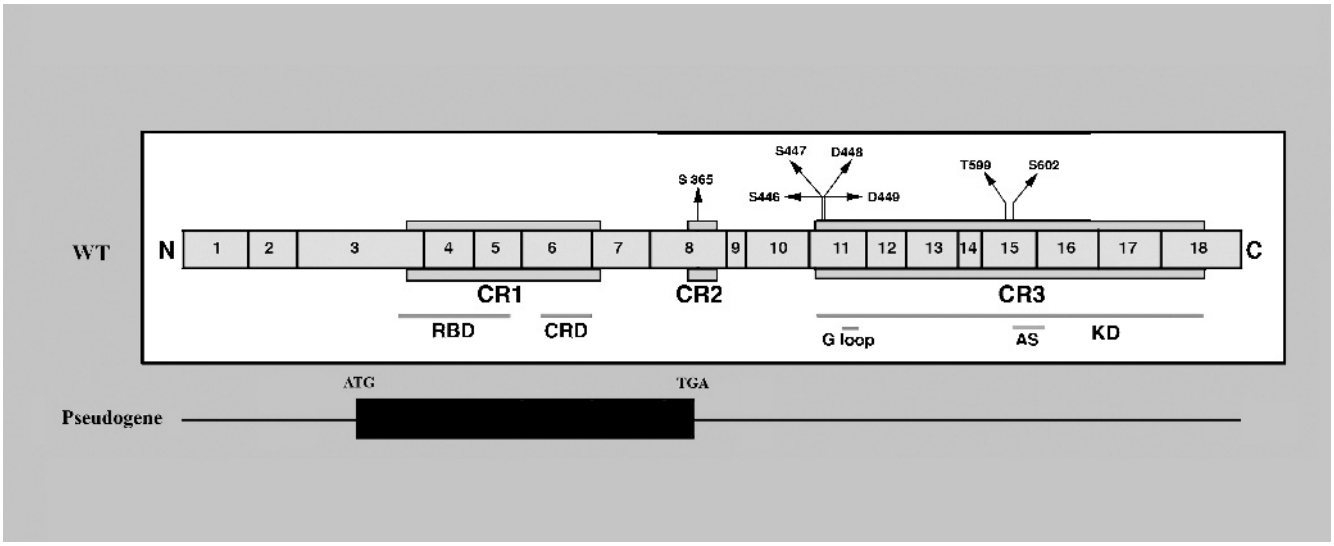

(B)

```
BRAF-wildtype:      MDTVTSSSSS SLSVL_____ __PSSLSVFQ NPTDVARSNP KSPQKPIVRV
BRAF-pseudogene:    MDTVKSSSSF SLSVFLFQFF KKPLSLSVFR NPIDVTWSNP KSPQKPIVRV

BRAF-wildtype:      FLPNKQRTVV PARVGVTVRD SLKKALMMRG LIPECCAVVR IQDGEKKPIG
BRAF-pseudogene:    FLPNKQRTVV PARCGVTVGD SLKKALMMRG LIPECGAVYR IQDGEKKTID

BRAF-wildtype:      WDTDISWLTG EELHVEVLEN VPLTTHNFVR KTFFTLAFCD FCRKLLFQGF
BRAF-pseudogene:    QDTGVSWLTG EELHVEVLEN VPLTTHNFVR KTFFTLAFCD FCQKLLFQGF

BRAF-wildtype:      RCQTCGYKFH QRCSTEVPLM CVNYDQLDLL FVSKFFEHHP IPQEEASLAE
BRAF-pseudogene:    RCQTCGYKFH QCCSTVVPLM FVNYDHLDLL FFSKFFERHS IPQEEASLAE

BRAF-wildtype:      TALTSGSSPS APASDSIGPQ ILTSPSPSKS IPIPQPFRPA DEDH
BRAF-pseudogene:    TALTSGSSPS APPSDSTGPQ ILTNLSPSKS TPIPQPFRPA DEDH*
```

Figure 5. (A) Schematic representation of human *BRAF* gene and its pseudogene in scale. Each *BRAF* exon is indicated by its number inside the boxes. The three conserved regions of the protein with the *ARAF* and *RAF-1* genes are indicated by CR1, CR2, and CR3, respectively. Ras binding domain (RBD), cysteine-rich domain (CRD), and kinase domain (KD) are indicated by three bars. G-loop is a conserved glycine motif in exon 11, and AS is the activation segment in exon 15. Black arrows indicate the major phosphorylation sites of the protein. The longest open reading frame of *BRAF* pseudogene is indicated by a black box and corresponds to wild type CR1 region, which plays a regulative role in kinase activity. (B) Amino acid sequence alignment between wild type *BRAF* and its pseudogene. Sequence difference is highlighted in bold. There are a total of 244 amino acids in the pseudogene coding region, and only 35 amino acid difference compared with wild type (85.68% homology).

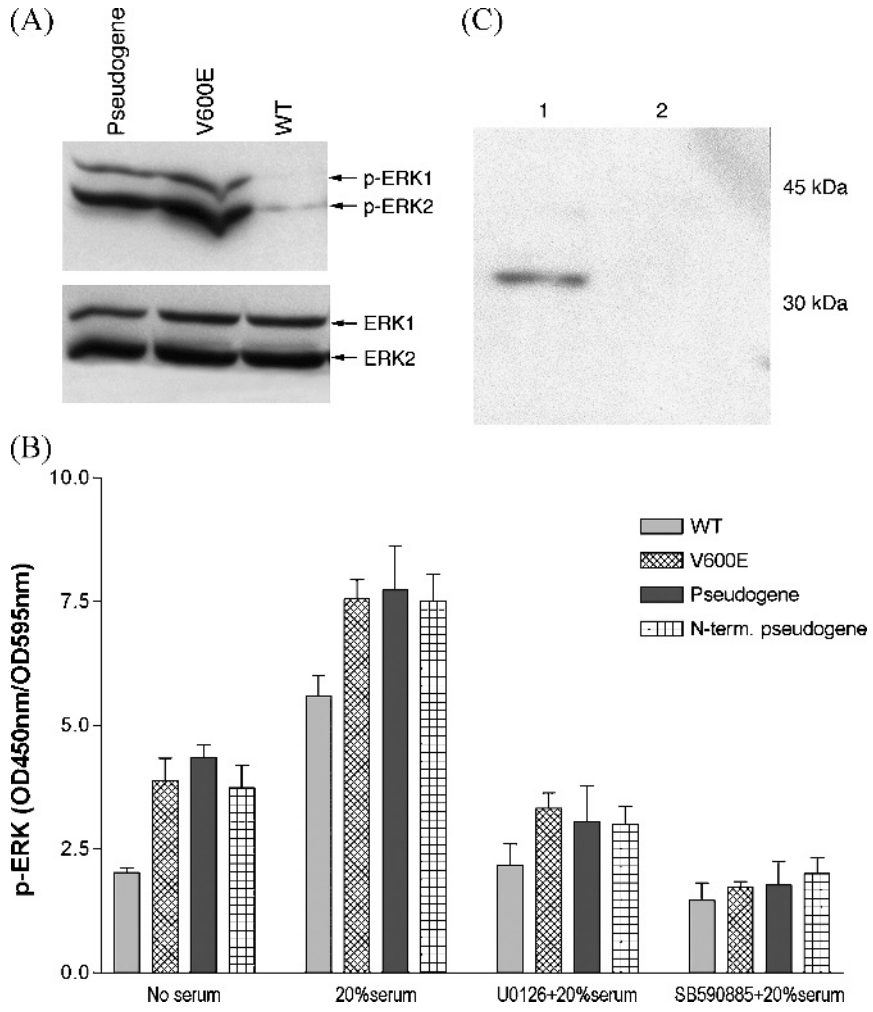

Figure 6. (A) Activation of MAP kinase by *BRAF* pseudogene. Chinese hamster ovary cells were stably transfected by pBRAF^{WT}, pBRAF^{V600E}, or pBRAF^{PSEUDO}, respectively. A total of 60 μg of proteins from each cell lysate were used for Western blot analysis. Two blots with identical amount of protein loading were probed with antibodies to phospho-ERK 1/2 (pERK, indicating MAP kinase activation) and total ERK 1/2 (for monitoring protein loading), respectively. (B) Quantification of MAP kinase activation by *BRAF* pseudogene and N-terminal part of *BRAF* pseudogene (pBRAF$^{PSEUDO\text{-}V5}$) in CHO cells. pBRAF^{PSEUDO}– and pBRAF$^{PSEUDO\text{-}V5}$–transfected CHO cells were cultured in serum-free medium for 16 hours. The cells were then stimulated with 20% fetal bovine serum for 2 hours in the presence or absence of 20 μM MEK inhibitor U0126 or BRAF inhibitor SB590885. The amount of phospho-ERK in the cells was measured using a cell-based ELISA kit at OD 450 nm and was normalized by dividing the OD 595 nm readings of relative cell number. Data are expressed as means ± SEM of two separate experiments. (C) Protein expression of *BRAF* pseudogene. The putative *BRAF* pseudogene coding region of 244 amino acids was cloned into a pcDNA3.1/V5-His vector (pBRAF$^{PSEUDO\text{-}V5}$) and was expressed as a fusion protein with a V5 epitope tag at the C-terminus in CHO cells. The expected 32-kDa fusion protein was detected by Western blot using V5 monoclonal antibody (lane 1). No protein was detected when CHO cells were transfected with a pcDNA3.1/V5-His vector alone (lane 2).

the N-terminal part of *BRAF* pseudogene. For confirmation that pseudogene transcripts could be translated into protein, we cloned the potential pseudogene coding sequence (244 amino acids N-terminus) into a pcDNA3.1/V5 expression vector in frame with the V5 epitope tag (pBRAF$^{PSEUDO\text{-}V5}$). Using V5 monoclonal antibody, we were able to detect a predicted 32-kDa protein in CHO cells stably transfected with the vector, whereas no protein was detected in CHO cells transfected with vector alone (Figure 6*C*).

The transformation potential of *BRAF* pseudogene was assessed *in vitro* by a soft agar assay in pBRAF^{PSEUDO}–transfected NIH3T3 and CHO cells and *in vivo* by subcutaneous injection of stably pBRAF^{PSEUDO}–transfected NIH3T3 cells into four nude mice. As shown in Figure 7, *A* and *B*, the soft agar assay resulted in six-fold increases in the number of colonies from pBRAF^{PSEUDO}–transfected NIH3T3 cells and a four-fold increase from pBRAF^{PSEUDO}–transfected CHO cells, respectively. All four nude mice developed tumors within 2 weeks after injection of 1×10^6 pBRAF^{PSEUDO}–transfected NIH3T3 cells.

Discussion

In the present study, we reported *BRAF* pseudogene expression in thyroid tumors, which could transactivate MAP kinase and induce tumors in nude mice. Furthermore, reciprocal *BRAF* mutation and its pseudogene expression were also demonstrated.

BRAF pseudogene is a processed pseudogene that arises by retrotransposition. In the process of retrotransposition, a portion of the mRNA transcript of a gene is spontaneously reverse-transcribed

back into DNA and inserted into chromosomal DNA. Because it is derived from a mature mRNA product, a processed pseudogene lacks introns and the upstream promoter of a normal gene and is thus considered "dead on arrival." Pseudogenes also have many genetic alterations such as point mutations, deletions, and insertions compared to their normal genes [22]. However, many exceptions exist where a pseudogene can be transcribed and even translated into an active protein [22–28]. Indeed, *BRAF* pseudogene produces mRNA transcripts that have many stop codons and cannot be translated into a functional, full-length protein. The longest open reading frame can only produce a polypeptide of 244 amino acids. This polypeptide has no kinase domain and, therefore, cannot be functional by itself. However, expression of *BRAF* pseudogene in some thyroid tumors suggests that it may play a role in thyroid tumor development. The functional studies confirmed that the *BRAF* pseudogene plays an oncogenic role in thyroid tumorigenesis by transactivating the MAP kinase pathway, likely through wild type BRAF, because BRAF inhibitor abolishes its effect. Given the high sequence homology between the CR1 domain of wild type *BRAF* and its pseudogene, it is likely that the *BRAF* pseudogene peptide interacts with the CR1 domain of wild type BRAF and interferes with its normal physiologic role of negatively autoregulating its C-terminal protein kinase domain. Hitotsune et al. [29,30] demonstrated that an expressed pseudogene Mkrn1-p1 could regulate the expression of its homologous functional coding gene by modulating messenger RNA stability. However, their results have been challenged recently by Gray et al. [31], who showed that the *Mkrn1-p1* pseudogene is neither expressed nor imprinted, nor does it transregulate its source gene. Apparently, the contradictory reports remain to be settled.

There is an inverse correlation between *BRAF* pseudogene activation and *BRAF* mutation in thyroid tumors. *BRAF* pseudogene transcripts are more frequently detected in benign goiters and early stages

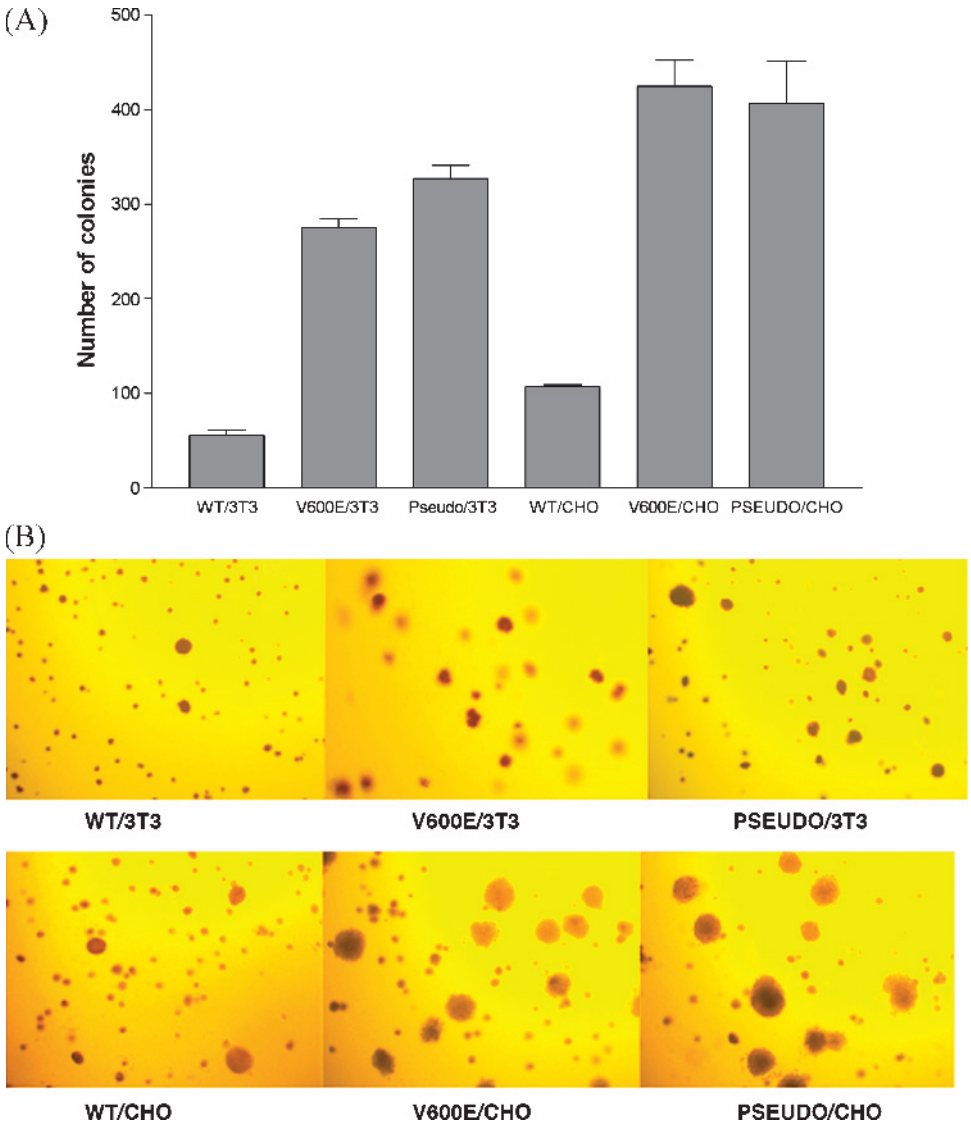

Figure 7. (A) Anchorage-independent growth of NIH3T3 and CHO cells stably transfected by pBRAF^{WT}, pBRAF^{V600E}, or pBRAF^{PSEUDO}, respectively. A total of 2×10^4 cells in 0.4% soft agar were cultured in duplicate in a six-well cell culture plate for 28 days. The colonies were stained and counted. The results are the average number of colonies per well from four wells. (B) Representative results of colony formation of NIH3T3 cells or CHO cells stably transfected by pBRAF^{WT}, pBRAF^{V600E}, or pBRAF^{PSEUDO}, respectively. Original magnification, ×40.

of thyroid cancer. It becomes silenced in late stages of cancer, especially when *BRAF* mutation is present, suggesting that only one of the events is enough to drive oncogenic transformation of normal thyroid epithelial cells. A previous study by Zhang et al. [32] showed that *PTEN* pseudogene expression might play a pathological role in glioblastomas and was complementary to PTEN mutation. In 14 of 18 glioblastomas, either *PTEN* mutation or *PTEN* pseudogene expression was found, and only one case showed both *PTEN* mutation and pseudogene expression. Their study reported similar observations to the current study, that is, *BRAF* or *PTEN* pseudogene expression could act as an alternative to *BRAF* or *PTEN* mutation [32].

The high frequency of *BRAF* pseudogene expression in benign goiters suggests that it may play a role in initiating goiter formation or that a subset of goiters may contain precursor lesions such as *BRAF* pseudogene expression, which may progress to malignancy in the context of additional genetic or environmental factors. Recent studies suggest that there may be abnormal *BRAF* in precursor lesions and *BRAF*E600 contributes to the formation of some benign lesions [33]. Our data suggest that the RAS-RAF-MEK-ERK-MAP kinase-signaling cascade may be involved in some benign thyroid goiters (43.8% in our study). Because the female-to-male ratio in thyroid epithelial cell tumors is 3:1, one may wonder whether *BRAF* pseudogene location on chromosome Xq13 contributes to this difference, although in female mammals, most genes on one X chromosome are silenced because of X-chromosome inactivation to achieve dosage compensation between males and females. However, recent studies have shown that some genes can escape X-inactivation and are expressed from both the active and inactive X chromosomes [34–36]. *BRAF* pseudogene may escape X-inactivation and remains active in some thyroid tumors. Further studies are needed to confirm this speculation. Finally, *BRAF* pseudogene expression in a subset of goiters may also have significant clinical implications. These patients may need to be followed up more closely for early sign of cancer development.

Acknowledgments

The authors thank Raafat M. El-Sayed from the Animal Facility for his excellent support.

Disclosure of conflicts of interest

All authors have nothing to declare.

References

[1] Hundahl SA, Fleming ID, Fremgen AM, and Menck HR (1998). A National Cancer Data Base report on 53,856 cases of thyroid carcinoma treated in the U.S., 1985–1995 [see comments]. *Cancer* **83**, 2638–2648.

[2] Kimura ET, Nikiforova MN, Zhu Z, Knauf JA, Nikiforov YE, and Fagin JA (2003). High prevalence of *BRAF* mutations in thyroid cancer: genetic evidence for constitutive activation of the RET/PTC-RAS-BRAF signaling pathway in papillary thyroid carcinoma. *Cancer Res* **63**, 1454–1457.

[3] Cohen Y, Xing M, Mambo E, Guo Z, Wu G, Trink B, Beller U, Westra WH, Ladenson PW, and Sidransky D (2003). *BRAF* mutation in papillary thyroid carcinoma. *J Natl Cancer Inst* **95**, 625–627.

[4] Soares P, Trovisco V, Rocha AS, Lima J, Castro P, Preto A, Maximo V, Botelho T, Seruca R, and Sobrinho-Simoes M (2003). *BRAF* mutations and RET/PTC rearrangements are alternative events in the etiopathogenesis of PTC. *Oncogene* **22**, 4578–4580.

[5] Namba H, Nakashima M, Hayashi T, Hayashida N, Maeda S, Rogounovitch TI, Ohtsuru A, Saenko VA, Kanematsu T, and Yamashita S (2003). Clinical implication of hot spot *BRAF* mutation, V599E, in papillary thyroid cancers. *J Clin Endocrinol Metab* **88**, 4393–4397.

[6] Xu X, Quiros RM, Gattuso P, Ain KB, and Prinz RA (2003). High prevalence of *BRAF* gene mutation in papillary thyroid carcinomas and thyroid tumor cell lines. *Cancer Res* **63**, 4561–4567.

[7] Xing M (2005). *BRAF* mutation in thyroid cancer. *Endocr Relat Cancer* **12**, 245–262.

[8] Fagin JA (2004). How thyroid tumors start and why it matters: kinase mutants as targets for solid cancer pharmacotherapy. *J Endocrinol* **183**, 249–256.

[9] Garnett MJ and Marais R (2004). Guilty as charged: *B-RAF* is a human oncogene. *Cancer Cell* **6**, 313–319.

[10] Davies H, Bignell GR, Cox C, Stephens P, Edkins S, Clegg S, Teague J, Woffendin H, Garnett MJ, Bottomley W, et al. (2002). Mutations of the *BRAF* gene in human cancer. *Nature* **417**, 949–954 (Epub 2002 Jun 2009).

[11] Wan PT, Garnett MJ, Roe SM, Lee S, Niculescu-Duvaz D, Good VM, Jones CM, Marshall CJ, Springer CJ, Barford D, et al. (2004). Mechanism of activation of the RAF-ERK signaling pathway by oncogenic mutations of *B-RAF*. *Cell* **116**, 855–867.

[12] Dhillon AS and Kolch W (2004). Oncogenic *B-Raf* mutations: crystal clear at last. *Cancer Cell* **5**, 303–304.

[13] Eychene A, Barnier JV, Apiou F, Dutrillaux B, and Calothy G (1992). Chromosomal assignment of two human *B-raf(Rmil)* proto-oncogene loci: *B-raf-1* encoding the p94Braf/Rmil and *B-raf-2*, a processed pseudogene. *Oncogene* **7**, 1657–1660.

[14] Mighell AJ, Smith NR, Robinson PA, and Markham AF (2000). Vertebrate pseudogenes. *FEBS Lett* **468**, 109–114.

[15] Zhang Z, Carriero N, and Gerstein M (2004). Comparative analysis of processed pseudogenes in the mouse and human genomes. *Trends Genet* **20**, 62–67.

[16] Tam OH, Aravin AA, Stein P, Girard A, Murchison EP, Cheloufi S, Hodges E, Anger M, Sachidanandam R, Schultz RM, et al. (2008). Pseudogene-derived small interfering RNAs regulate gene expression in mouse oocytes. *Nature* **453**, 534–538.

[17] Sasidharan R and Gerstein M (2008). Genomics: protein fossils live on as RNA. *Nature* **453**, 729–731.

[18] Piehler AP, Hellum M, Wenzel JJ, Kaminski E, Haug KB, Kierulf P, and Kaminski WE (2008). The human ABC transporter pseudogene family: evidence for transcription and gene-pseudogene interference. *BMC Genomics* **9**, 165.

[19] Greene FL, Page DL, Fleming ID, Fritz AG, Balch CM, Haller DG, and Morrow M (2002). Thyroid. In *American Joint Committee on Cancer: AJCC Cancer Staging Manual*, 6th ed. New York, NY: Springer, pp. 77–87.

[20] Shi Y, Zou M, Baitei EY, Alzahrani AS, Parhar RS, Al-Makhalafi Z, and Al-Mohanna FA (2008). Cannabinoid 2 receptor induction by IL-12 and its potential as a therapeutic target for the treatment of anaplastic thyroid carcinoma. *Cancer Gene Ther* **15**, 101–107.

[21] Chong H and Guan KL (2003). Regulation of Raf through phosphorylation and N terminus–C terminus interaction. *J Biol Chem* **278**, 36269–36276.

[22] Balakirev ES and Ayala FJ (2003). Pseudogenes: are they "junk" or functional DNA? *Annu Rev Genet* **37**, 123–151.

[23] Renaudie F, Yachou AK, Grandchamp B, Jones R, and Beaumont C (1992). A second ferritin L subunit is encoded by an intronless gene in the mouse. *Mamm Genome* **2**, 143–149.

[24] Sorge J, Gross E, West C, and Beutler E (1990). High level transcription of the glucocerebrosidase pseudogene in normal subjects and patients with Gaucher disease. *J Clin Invest* **86**, 1137–1141.

[25] Kandouz M, Bier A, Carystinos GD, Alaoui-Jamali MA, and Batist G (2004). *Connexin43* pseudogene is expressed in tumor cells and inhibits growth. *Oncogene* **23**, 4763–4770.

[26] Chakrabarti R, McCracken JB Jr, Chakrabarti D, and Souba WW (1995). Detection of a functional promoter/enhancer in an intron-less human gene encoding a glutamine synthetase–like enzyme. *Gene* **153**, 163–199.

[27] Sun D, Elsea SH, Patel PI, and Funk CD (1998). Cloning of a human "epidermal-type" 12-lipoxygenase–related gene and chromosomal localization to 17p13. *Cytogenet Cell Genet* **81**, 79–82.

[28] Thiele H, Berger M, Skalweit A, and Thiele BJ (2000). Expression of the gene and processed pseudogenes encoding the human and rabbit translationally controlled tumour protein (TCTP). *Eur J Biochem* **267**, 5473–5481.

[29] Hirotsune S, Yoshida N, Chen A, Garrett L, Sugiyama F, Takahashi S, Yagami K, Wynshaw-Boris A, and Yoshiki A (2003). An expressed pseudogene regulates

the messenger-RNA stability of its homologous coding gene. *Nature* **423**, 91–96.

[30] Yano Y, Saito R, Yoshida N, Yoshiki A, Wynshaw-Boris A, Tomita M, and Hirotsune S (2004). A new role for expressed pseudogenes as ncRNA: regulation of mRNA stability of its homologous coding gene. *J Mol Med* **82**, 414–422.

[31] Gray TA, Wilson A, Fortin PJ, and Nicholls RD (2006). The putatively functional *Mkrn1-p1* pseudogene is neither expressed nor imprinted, nor does it regulate its source gene *in trans*. *Proc Natl Acad Sci USA* **103**, 12039–12044.

[32] Zhang CL, Tada M, Kobayashi H, Nozaki M, Moriuchi T, and Abe H (2000). Detection of PTEN nonsense mutation and psiPTEN expression in central nervous system high-grade astrocytic tumors by a yeast-based stop codon assay. *Oncogene* **19**, 4346–4353.

[33] Michaloglou C, Vredeveld LC, Mooi WJ, and Peeper DS (2008). BRAF(E600) in benign and malignant human tumours. *Oncogene* **27**, 877–895.

[34] Brown CJ and Greally JM (2003). A stain upon the silence: genes escaping X inactivation. *Trends Genet* **19**, 432–438.

[35] Carrel L and Willard HF (2005). X-inactivation profile reveals extensive variability in X-linked gene expression in females. *Nature* **434**, 400–404.

[36] Disteche CM, Filippova GN, and Tsuchiya KD (2002). Escape from X inactivation. *Cytogenet Genome Res* **99**, 36–43.